ADVANCED FUNCTIONAL MATERIALS

Supporting Information

for *Adv. Funct. Mater.*, DOI: 10.1002/adfm.202009104

Ligand-Programmed Consecutive Symmetry Break(s) in Nanoparticle Based Materials Showing Emergent Phenomena: Transitioning from Sixfold to Threefold Symmetry in Anisotropic ZnO Colloids

*Sebastian Theiss, Michael Voggel, Henning Kuper, Martin Hoermann, Ulrich Krings, Peter Baum, Joerg August Becker, Valentin Witmann, and Sebastian Polarz**

Ligand-Programmed Consecutive Symmetry Break(s) in Nanoparticle Based Materials Showing Emergent Phenomena: Transitioning from Six-Fold to Three-Fold Symmetry in Anisotropic ZnO Colloids

Sebastian Theiss,[a,b] Michael Voggel,[b] Henning Kuper,[c] Martin Hoermann,[b] Ulrich Krings,[d] Peter Baum,[b] Joerg August Becker,[c] Valentin Wittman,[b] and Sebastian Polarz [a,b,]*

(a) S. Theiss, Prof. Dr. S. Polarz
Leibniz-University of Hannover, Institute of Inorganic Chemistry, Callinstrasse 9, 30167 Hannover, Germany
E-mail: sebastian.polarz@aca.uni-hannover.de

(b) S. Theiss, M. Voggel, M. Hoermann, Prof. Dr. P. Baum, Prof. Dr. V. Wittmann
University of Konstanz, Universitaetsstrasse 10, 78457 Konstanz, Germany

(c) H. Kuper, Prof. Dr. J. Becker
Leibniz-University of Hannover, Institute of Physical Chemistry, Callinstrasse 3A, 30167 Hannover, Germany

(d) Dr. U. Krings
Leibniz-University of Hannover, Institute of Food Chemistry, Callinstrasse 3-9, 30167 Hannover, Germany

ELECTRONIC SUPPLEMENTARY INFORMATION

Fig. S1:

a) PXRD measurement of the trigonal ZnO nanoparticles

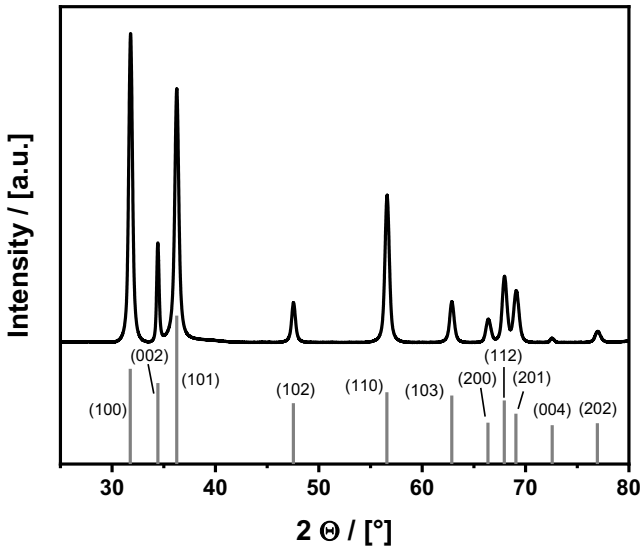

b) DLS Measurement of a dispersion of the trigonal ZnO nanorods in cyclohexane

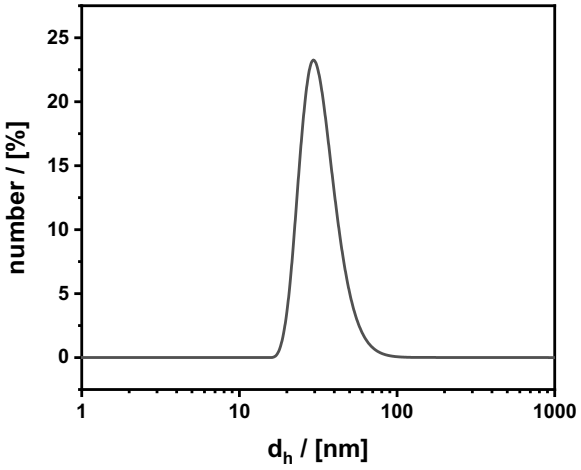

c) Evaluation of polydispersity and aspect ratio of trigonal ZnO nanorods

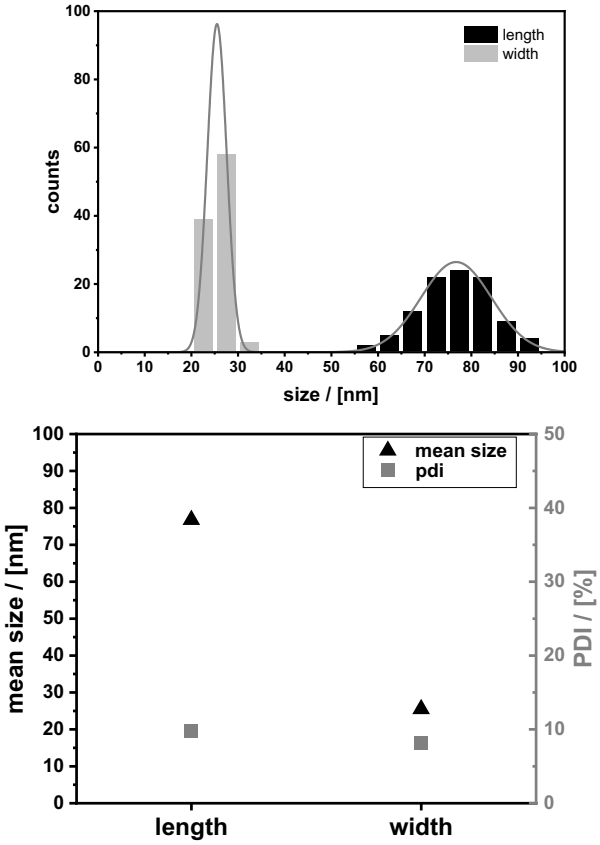

d) UV-Vis spectra of triangular ZnO nanorods

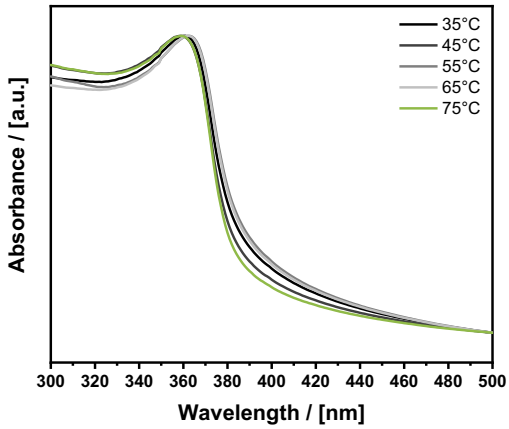

Fig- S2:

Lewis-Structures of Polyglyceryl-3-polyricinoleate (P3P) as well as Glycerol-monooleate (Mono-Ol), 1,3-Glycerol-dioleate (Di-Ol) and Glycerol-trioleate (Tri-Ol):

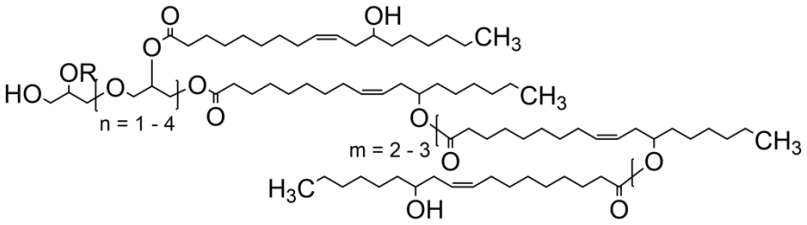

P3P

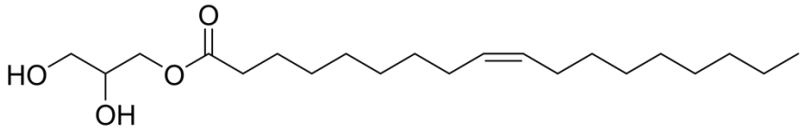

Mono-Ol

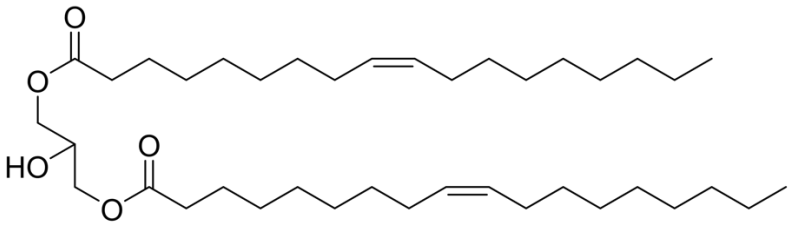

Di-Ol

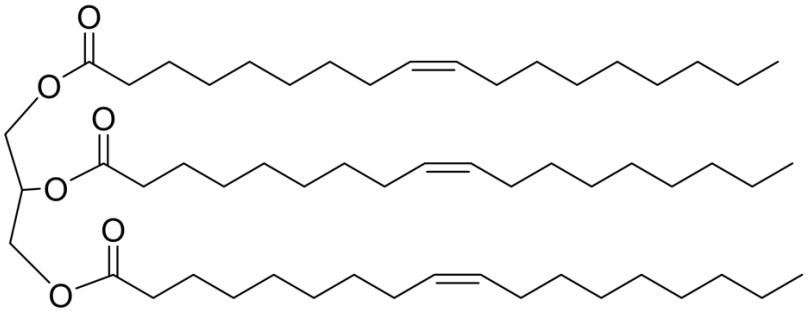

Tri-Ol

Fig. S3:

Normalized **IR** spectra of ZnO nanoparticles synthesized with pure Mono-Ol a), pure Di-Ol b), and pure Tri-Ol c), each for three identical washing cycles:

a)

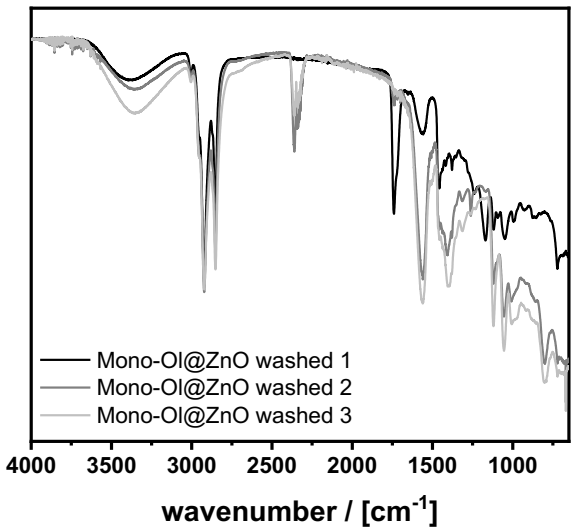

~3500-3200 cm^{-1}: O-H stretching bond of residual water; **3000-2800 cm^{-1}**: aliphatic C-H stretching bond; **~2300 cm^{-1}**: C=C stretching bond; **1739 cm^{-1}**: non-coordinated carbonyl stretching bond, C=O; **1560 cm^{-1}**: shifted, coordinated carbonyl stretching bond; **1400 cm^{-1}**: asymmetric C-H bending; **1300-1000 cm^{-1}**: aliphatic C-O ester stretching bond.

b)

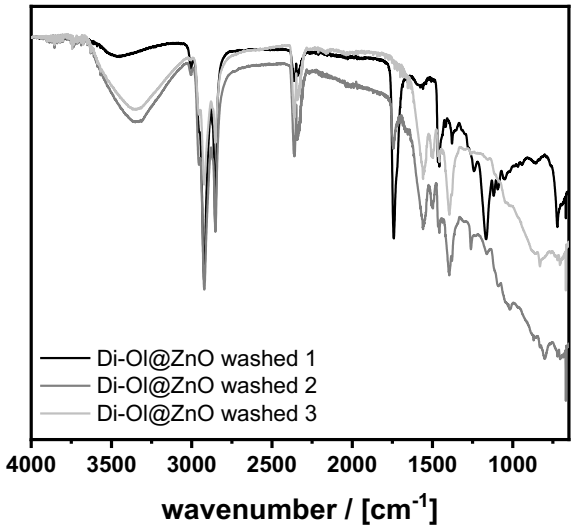

~3500-3200 cm^{-1}: O-H stretching bond of residual water; **3000-2800 cm^{-1}**: aliphatic C-H stretching bond; **~2300 cm^{-1}**: C=C stretching bond; **1740 cm^{-1}**: non-coordinated carbonyl stretching bond, C=O; **1557 cm^{-1}**: shifted, coordinated carbonyl stretching bond; **1394 cm^{-1}**: asymmetric C-H bending; **1300-1000 cm^{-1}**: aliphatic C-O ester stretching bond.

c)

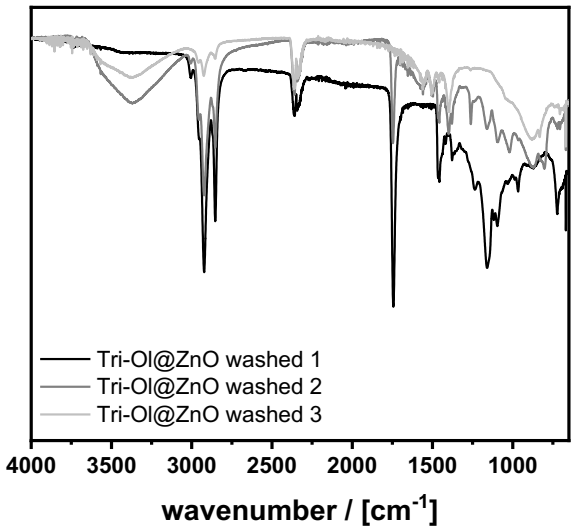

~3500-3200 cm^{-1}: O-H stretching bond of residual water; **3000-2800 cm^{-1}**: aliphatic C-H stretching bond; **~2360 cm^{-1}**: C=C stretching bond; **1743 cm^{-1}**: non-coordinated carbonyl stretching bond, C=O; **1560 cm^{-1}**: shifted, coordinated carbonyl stretching bond; **1394 cm^{-1}**: asymmetric C-H bending; **1300-1000 cm^{-1}**: aliphatic C-O ester stretching bond.

d)

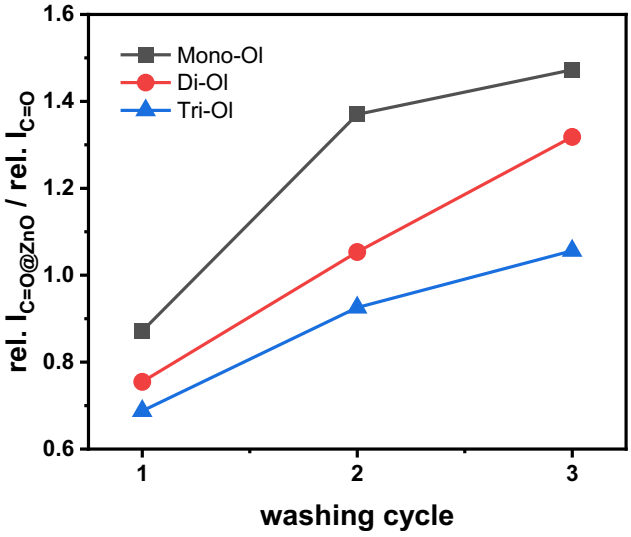

Ratios of the normalized relative intensities of coordinated and non-coordinated C=O stretching bonds of all three ligands (Mono-, Di-, and Tri-OI), each for three identical washing cycles:

e)

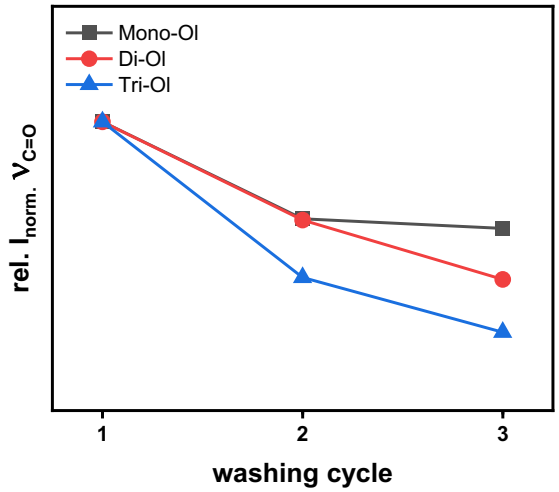

f)

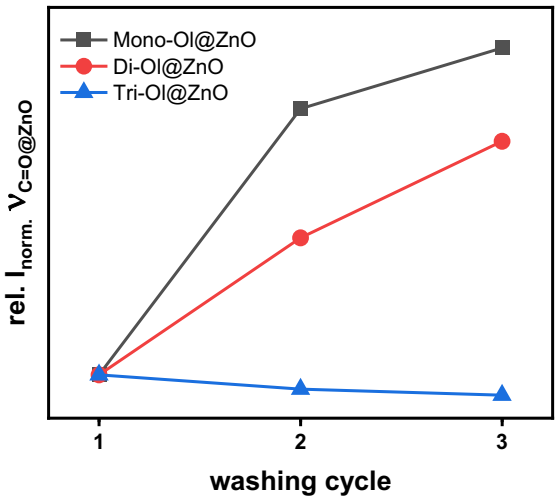

Normalized relative intensities of the free and coordinated C=O-stretching bonds of the three ligands Mono-Ol, Di-Ol and Tri-Ol, each for three identical washing cycles:

Table S1: Molar ratios of the different glycerol ligands and corresponding values of $Q_{morph.}$

Sample	$X_{Mono\text{-}Ol}$ [mol%]	$X_{Di\text{-}Ol}$ [mol%]	$X_{Tri\text{-}Ol}$ [mol%]	$Q_{morph.}$
1	100	0	0	0.05037
2	0	100	0	--
3	0	0	100	--
4	33.3	33.3	33.3	0.02255
5	50	50	0	0.04685
6	80	20	0	0.10877
7	70	30	0	0.14336
8	65	27.85	7.15	0.06765
9	42	58	0	1
10	40	17.15	42.85	0.0397
11	40	45	15	0.08307
12	30	70	0	0

Fig S4:

a)

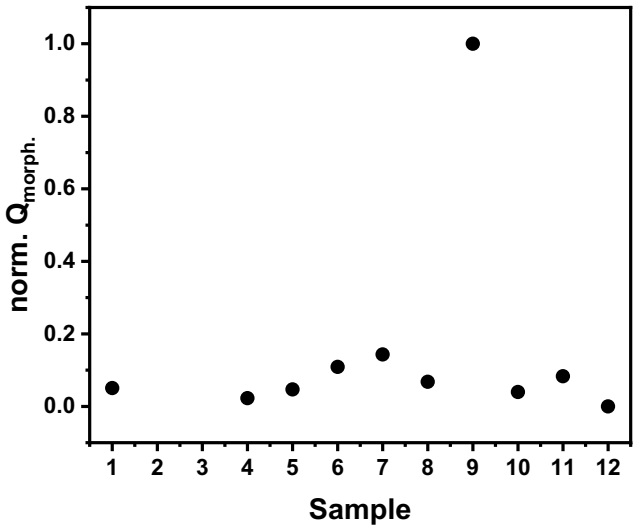

Normalized plot of $Q_{morph.}$ of the different molar compositions of the glycerol ligands presented in Table S1.

b) TEM images of ZnO samples, synthesized with different compositions of glycerol ligands as presented in Table S1.

Sample 1:

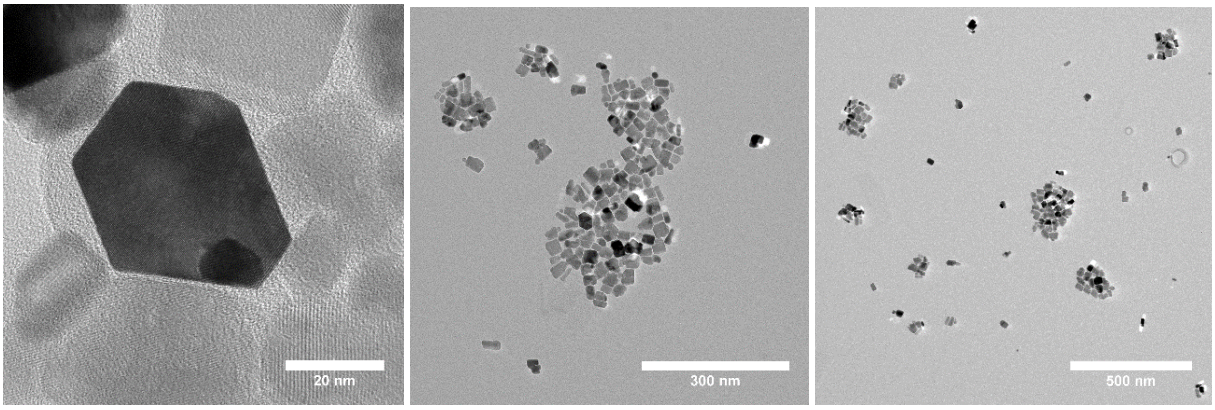

Sample 2:

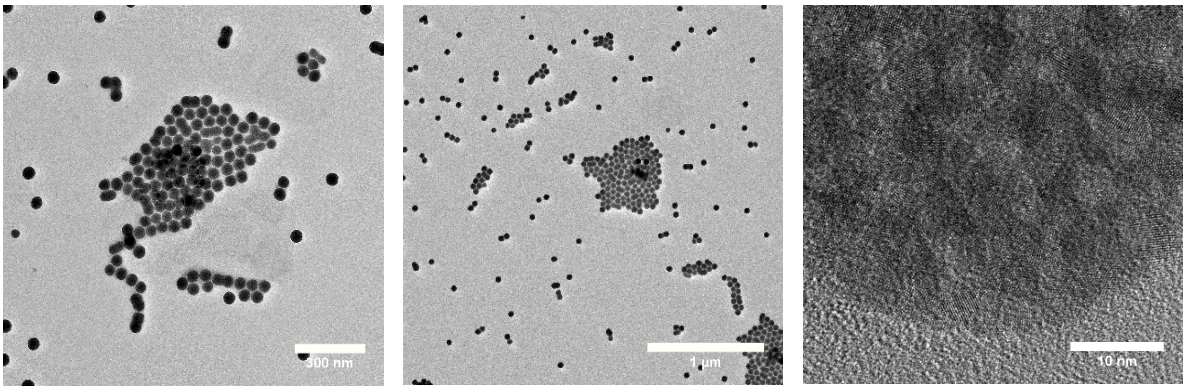

Sample 3:

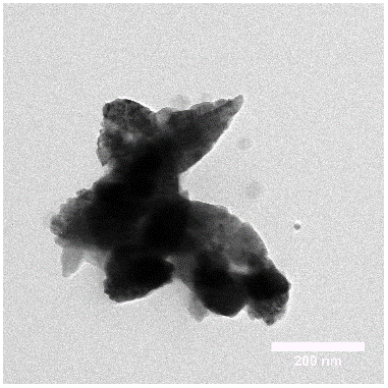

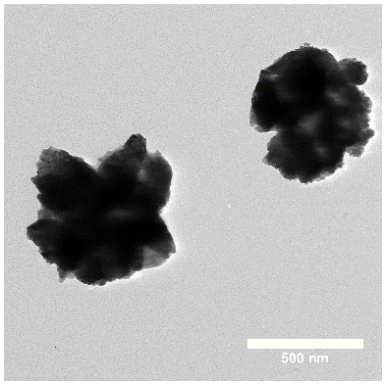

Sample 4:

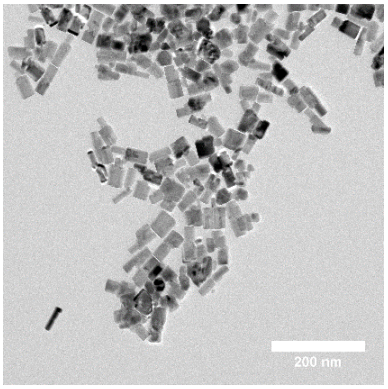

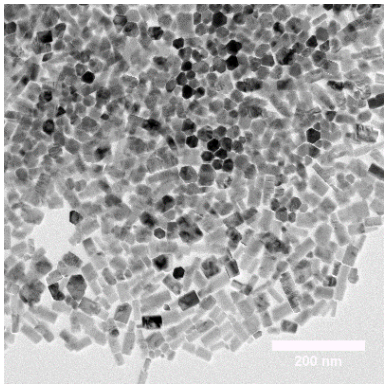

Sample 5:

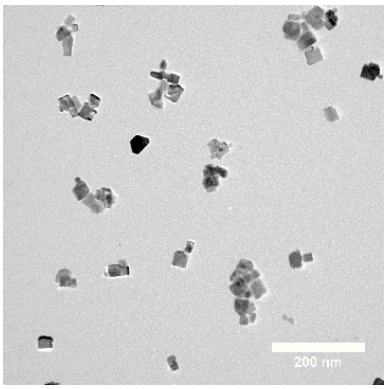

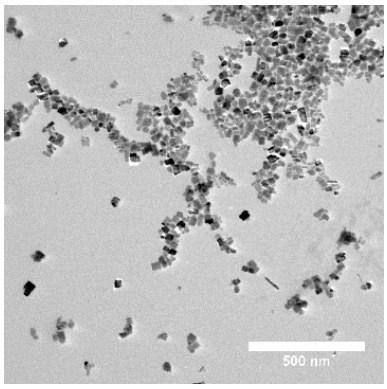

Sample 6:

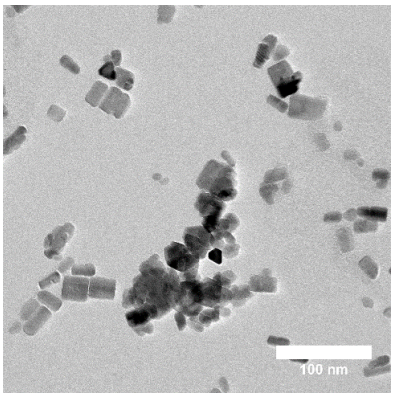

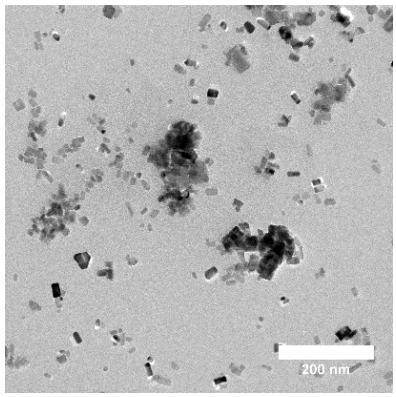

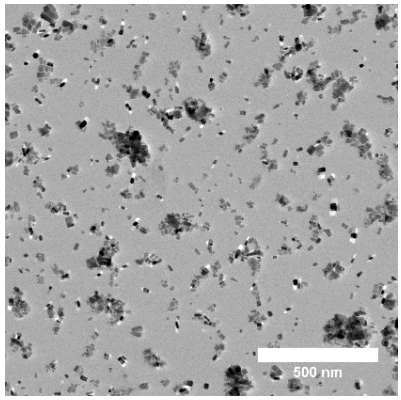

Sample 7:

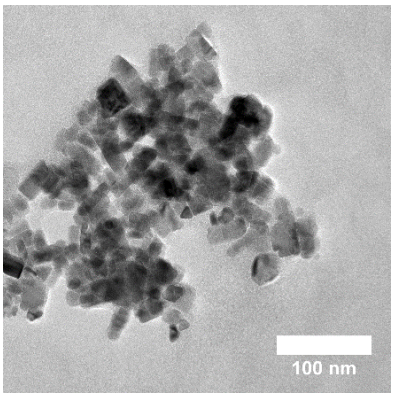

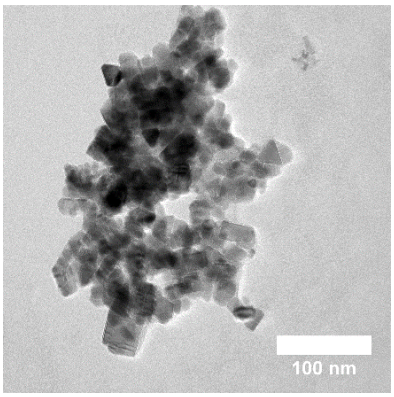

Sample 8:

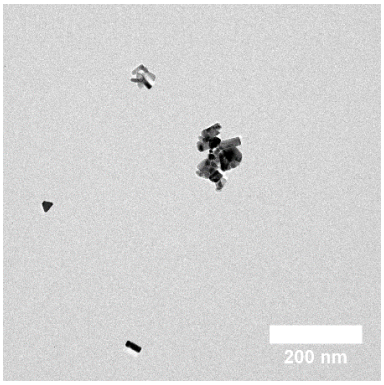

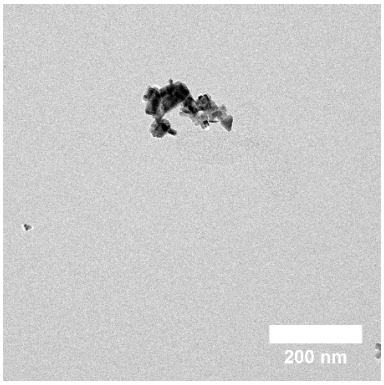

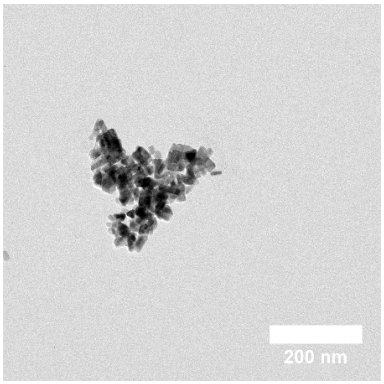

Sample 9:

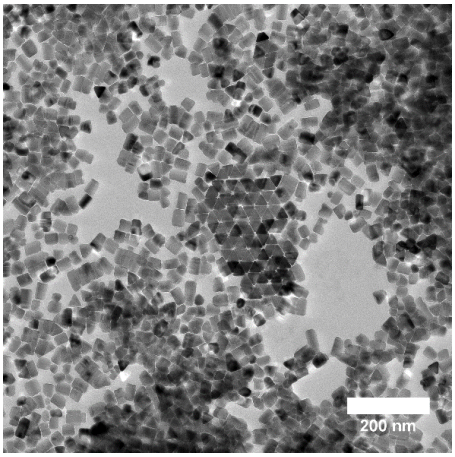

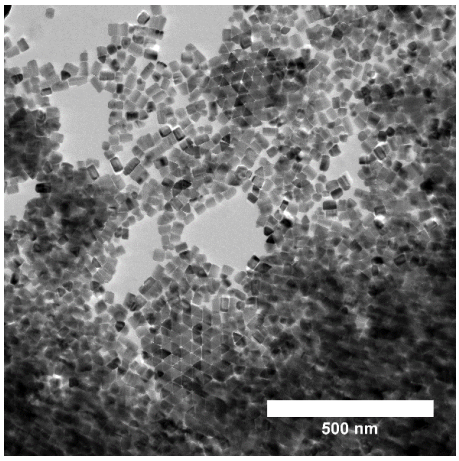

Sample 10:

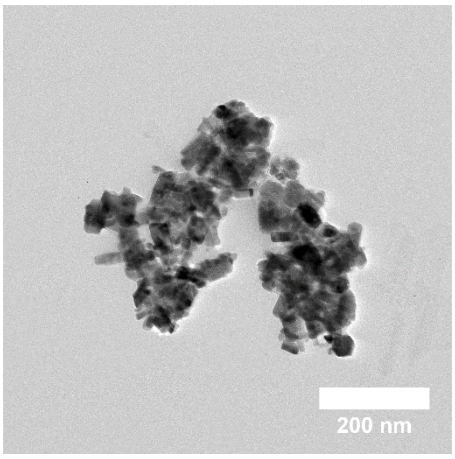

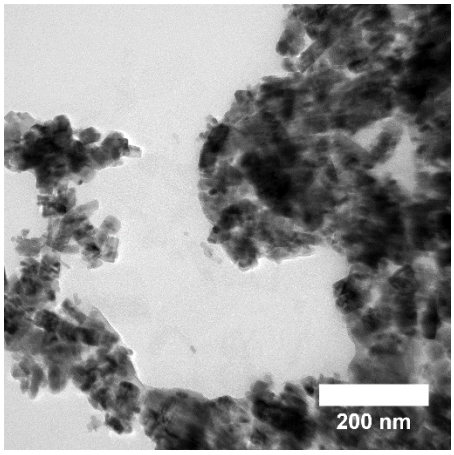

Sample 11:

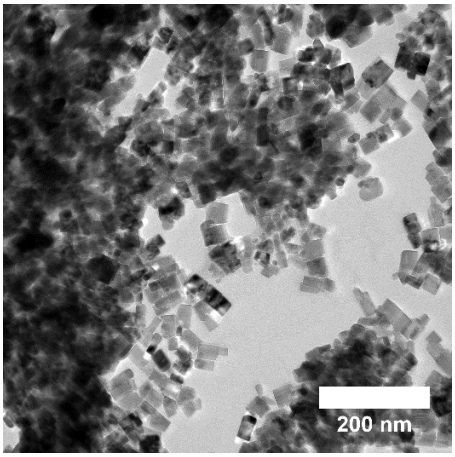

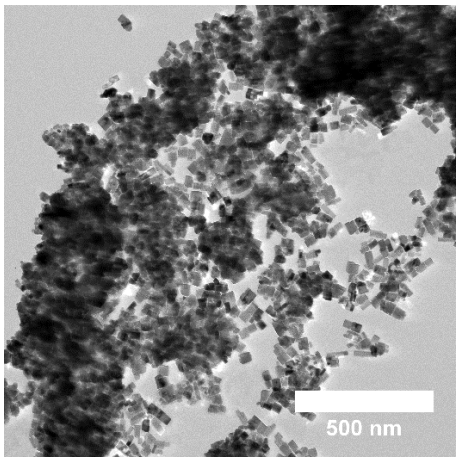

Sample 12:

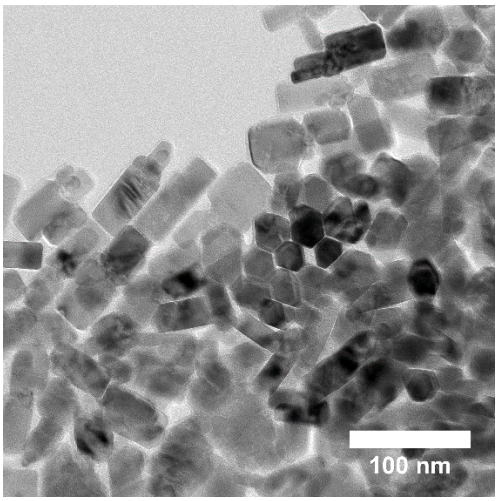

c)

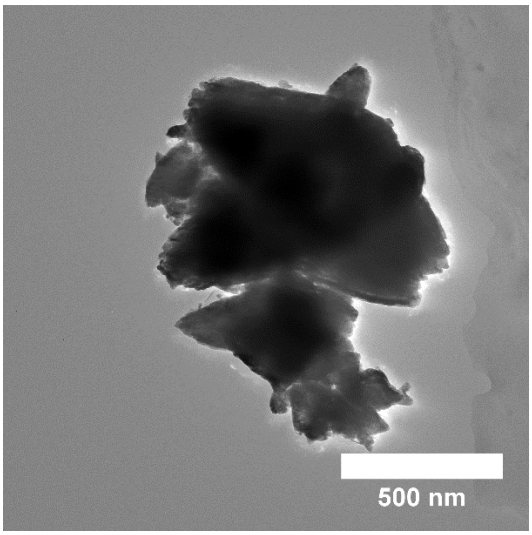

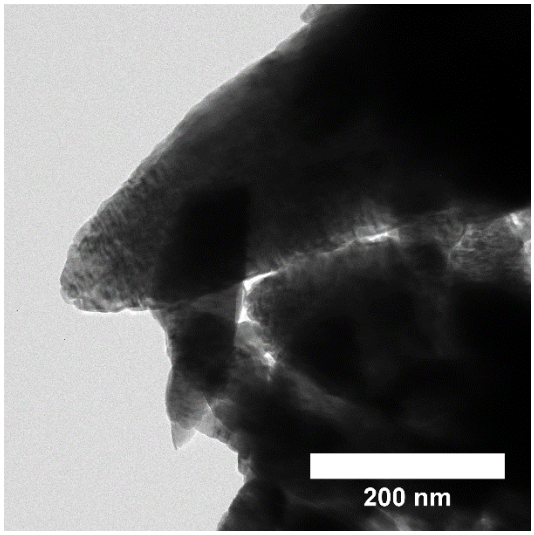

TEM images of ZnO particles, synthesized without any of the three ligands.

Fig S5:

a)

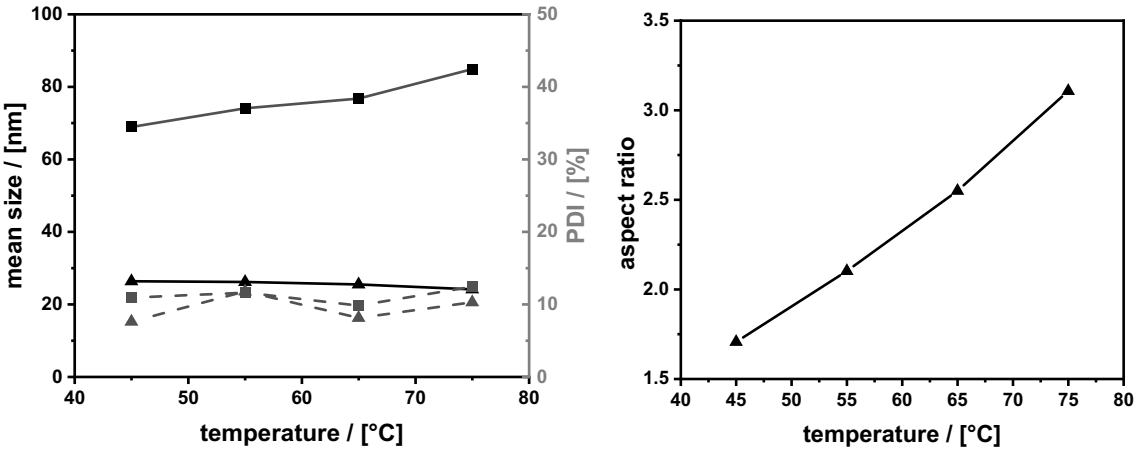

Influence of the temperature on the dimensions and the polydispersity of the nanoparticles during the synthesis; squares implicate the length (*c*), triangles implicate the width (*a,b*) of the nanoparticles.

b)

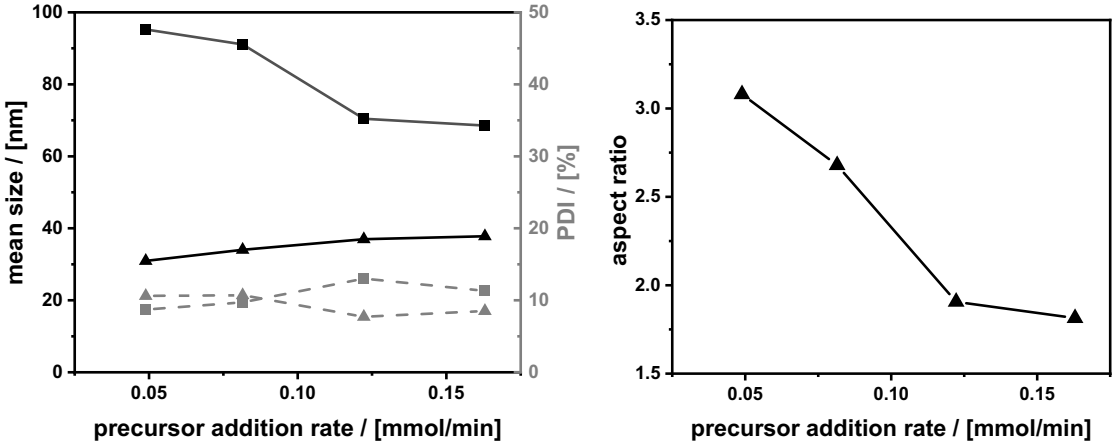

Influence of the precursor addition rate on the dimensions and the polydispersity of the nanoparticles during the synthesis; squares implicate the length (*c*), triangles implicate the width (*a,b*) of the nanoparticles.

Fig. S6:

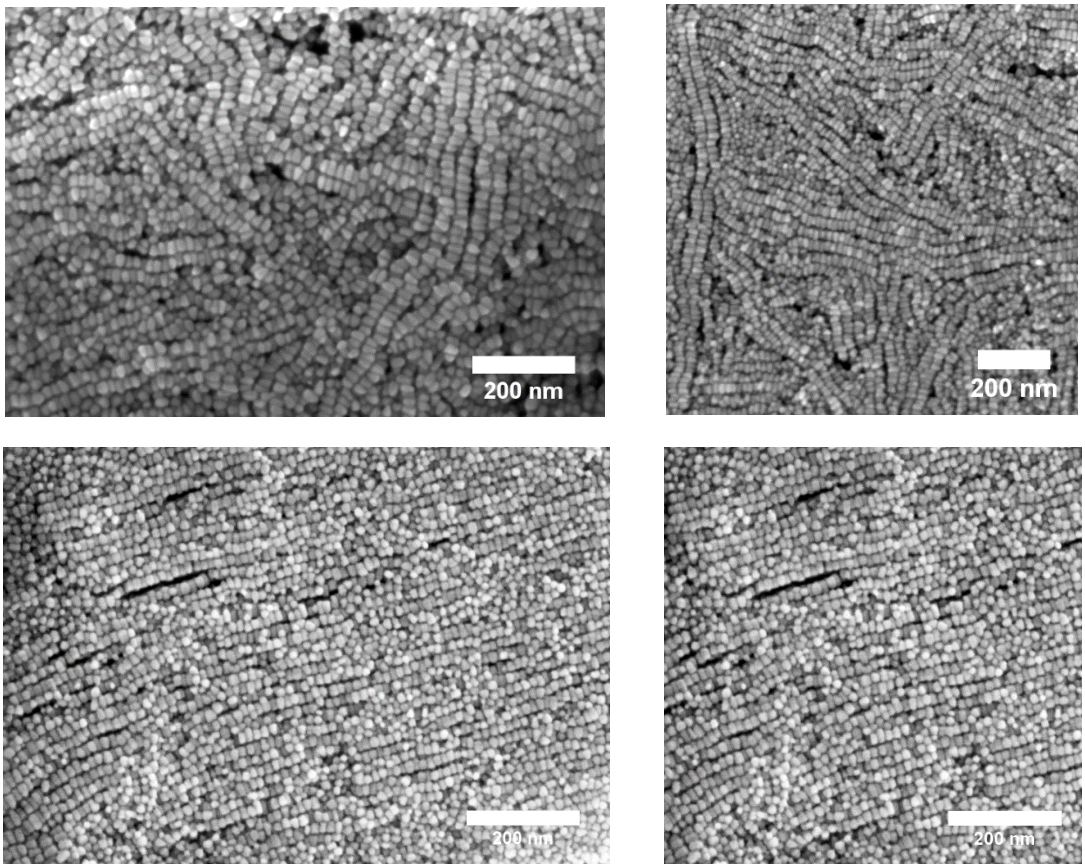

Side-view SEM images of superstructures of ZnO nanoparticles. The particles form ladder-like arrays spanning over several hundred nanometres.

Fig. S7:

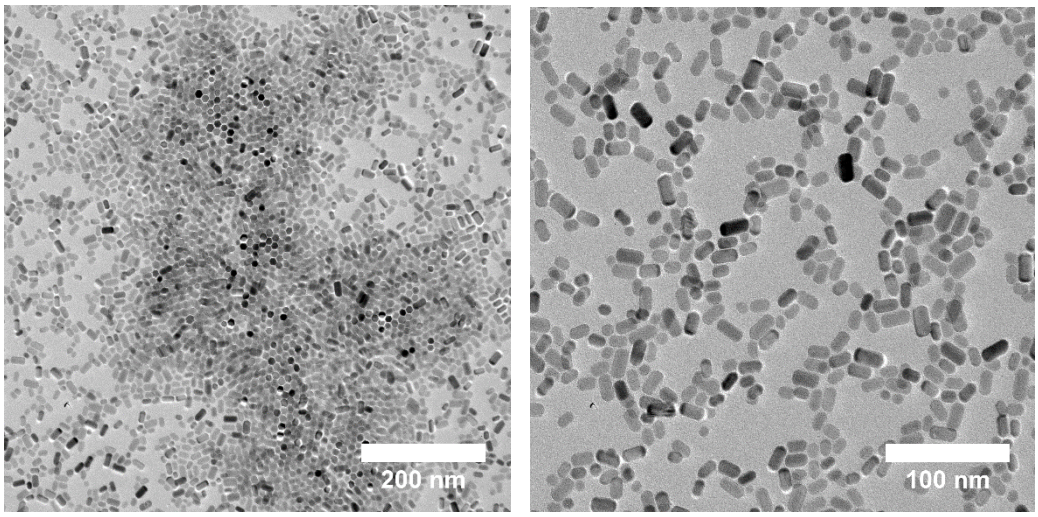

TEM images of ZnO nanorods (hexagonal).